Flying-start Strategy for Permanent-Magnet-Synchronous-Motor Under Position Sensorless Control with Initial Speed Estimation

Rongjiao Hao, Shinji Doki [1)] Kazuki Asahina, Akira Ide [2)]

1) Nagoya University, Furo-cho, Chikusa-ku, Nagoya, Aichi, 464-8603, Japan

E-mail: hao.rongjiao0112@nagoya-u.jp, doki@nagoya-u.jp

2) Toyota Industries Corporation, Toyoda-cho, Kariya-shi, Aichi, 448-8671, Japan

E-mail: kazuki.asahina@mail.toyota-shokki.co.jp, akira.ide@mail.toyota-shokki.co.jp

ABSTRACT: In this paper, a flying-start strategy for position-sensorless-controlled permanent-magnet-synchronous-motor (PMSM) with the initial speed estimation is proposed. For the motors with lower rated speed, initial position estimation based on Extended Electromotive Force(EEMF) is fast enough for flying-start, but proper current control cannot be guaranteed if it comes to higher speed, unless both the speed and position are fully estimated. In the proposed method, the initial speed of the motor is estimated in a short time to improve the position estimation and decrease the decoupling voltage error during the flying-start at middle or high speed.

KEY WORDS: Extended electro-motive force, Flying-start, Permanent-magnet-synchronous-machine(PMSM), Sensorless control

1. INTRODUCTION

Since the temperature problems have become one of the most important issues globally, the attention paid to the electric vehicles (EV) are developing rapidly. Permanent-magnet synchronous motors(PMSM) are widely used in these vehicles due to their high efficiency and high power density. As a method to realize lower cost and higher reliability, position sensorless techniques have grabbed people's attention, and have been investigated for three decades. [(1)(2)(3)(4)(5)]

However there are still some issues should be considered, and one of them is flying-start. Flying-start means that FOC is initialized during rotation, which needs initial position to initialize voltage reference of the inverter for suppressing inrush current caused by back-EMF. Therefore, the response of initial position estimation is important for flying-start under position sensorless control. One conventional approach is injecting a high-frequency voltage to detect the saliency, but this can only be applied at low speed.[(6)] Most of recent strategies are applying zero-volatge vector pulses intermittently to estimate the initial position.[(7)] These strategies are generally complicated, sensitive to speed variations. Otherwise, most of them have not discussed about the importance of the initial speed estimation, which makes it difficult for these strategies to startup from high speed.

In our previous research, a flying-start strategy for over-all speed with Extended Electromotive Force(EEMF) is proposed,[(8)] avoiding the inrush current with the quick response of the initial position estimation. But if it comes to higher rated speed, it is clear that the initial speed estimation becomes more important.

In this paper, the importance of the initial speed estimation for flying-start strategy is discussed, and a simple improved flying-start strategy with the initial speed estimation is proposed. Finally the performance evaluation experiments' results are reported.

2. INITIAL SPEED ESTIMATION

2.1. The issues on the conventional flying-start strategy

In our previous research, a flying-start strategy with Extended Electromotive Force(EEMF) is proposed, avoiding the inrush current with the quick response of the initial position estimation by EEMF. [(3)] The reason of the quick response is explained by the EEMF estimation model below.

$$\begin{bmatrix}\hat{e}_{\alpha_\omega}\\ \hat{e}_{\beta_\omega}\end{bmatrix} = \begin{bmatrix}v_\alpha^*\\ v_\beta^*\end{bmatrix} - \{(R+pL_d)\boldsymbol{I} + \hat{\omega}_{re}(L_q - L_d)\boldsymbol{J}\}\begin{bmatrix}i_\alpha\\ i_\beta\end{bmatrix} \quad (1)$$

$$\hat{\theta}_{re} = \tan^{-1}\left(\frac{-\hat{e}_{\alpha_\omega}}{\hat{e}_{\beta_\omega}}\right) \quad (2)$$

$$\boldsymbol{I} = \begin{bmatrix}1 & 0\\ 0 & 1\end{bmatrix},\ \boldsymbol{J} = \begin{bmatrix}0 & -1\\ 1 & 0\end{bmatrix}$$

During flying start, the initial voltage reference of the inverter is zero$(v_\alpha^* = v_\beta^* = 0)$, so actually real initial EEMF vector is the sum of current vector proportional to impedance and orthogonal velocity component vector, as shown in Eq.(3) and Fig. 1.

$$\begin{bmatrix}e_{\alpha_\omega}\\ e_{\beta_\omega}\end{bmatrix} = -\{(R+pL_d)\boldsymbol{I} + \omega_{re}(L_q - L_d)\boldsymbol{J}\}\begin{bmatrix}i_\alpha\\ i_\beta\end{bmatrix} \quad (3)$$

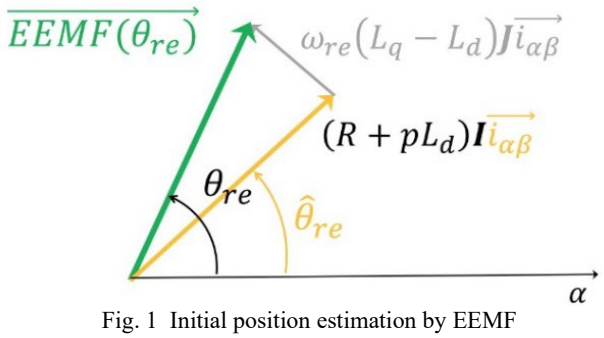

Fig. 1 Initial position estimation by EEMF

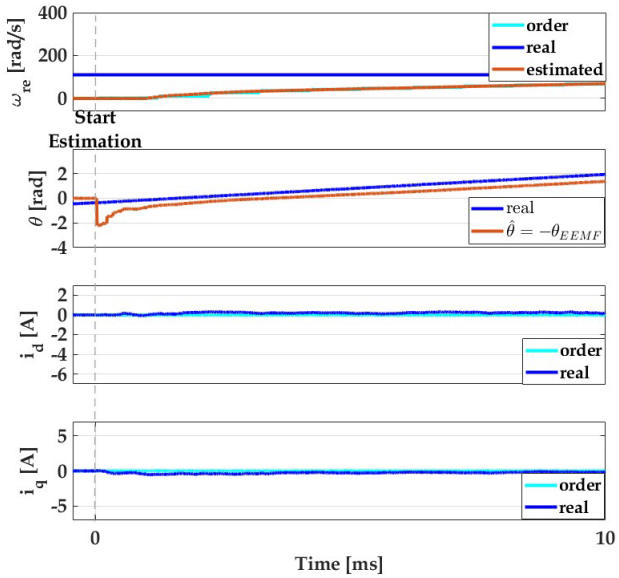

Fig. 2 Flying-start from middle speed with conventional speed estimation

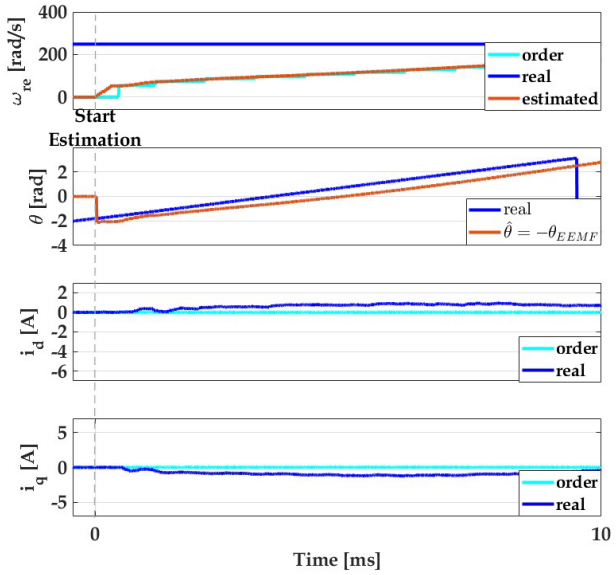

Fig. 3 Flying-start from high speed with conventional speed estimation

$$\begin{bmatrix} \hat{e}_{\alpha\omega} \\ \hat{e}_{\beta\omega} \end{bmatrix} = -(R + pL_d)\boldsymbol{I}\begin{bmatrix} i_\alpha \\ i_\beta \end{bmatrix} \quad (4)$$

Meanwhile, since initial estimated speed is zero, the estimated EEMF can be shown as Eq.(4), the yellow vector in Fig.1, which means the estimated position is the phase of current. When the

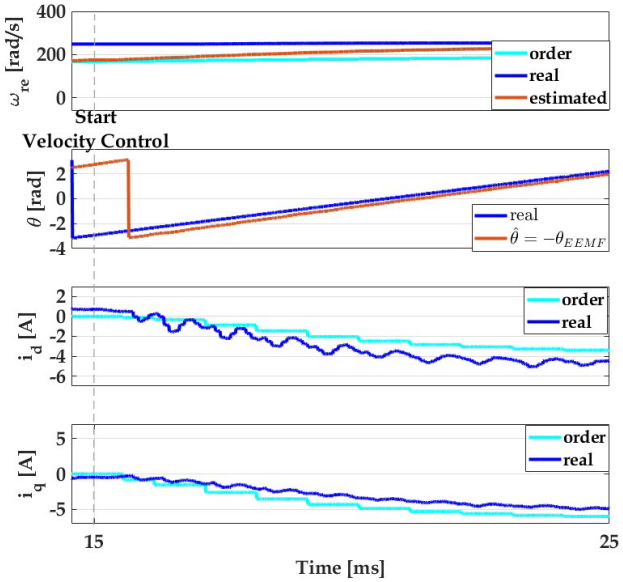

Fig. 4 Velocity Control after Flying-start from high speed with conventional speed estimation

velocity component vector is small, the estimated position can have an initial response with high accuracy, avoiding overcurrent during the flying start like Fig.2.

However, if it comes to higher speed, it is confirmed that the response of current control during startup becomes worse even the initial position estimation is fast like the experiment result in Fig.3. Otherwise, the position estimation also becomes worse after the initial response. Furthermore, the appropriate velocity control cannot be performed after flying-start with the conventional speed estimation like Fig.4 .

And it is clear that besides to estimated position, the second input to the current controller, the initial value response of the estimated speed $\hat{\omega}_{re}$ causes the disturbance to the controller and the estimator. Normally, the motor speed can be estimated by the differential of the estimated position $\hat{\theta}_{re}$ with a first-order low-pass filter. Since the time constant of speed estimation is limited by the observer filter, the speed estimation error may lead to overcurrent, even the initial position estimation can suppress it shortly like Fig.1. Therefore, a quick initial speed estimation is needed for flying-start.

2.2. Initial speed estimation method

In the proposed method, an approximate value of the initial speed is estimated just like the initial position estimation by EEMF in Fig.2. The estimated EEMF vector without considering the velocity component vector is defined as the Approximate Electromotive Force $\boldsymbol{e_0}$, and the approximate value of the initial speed can be estimated by the equation below.

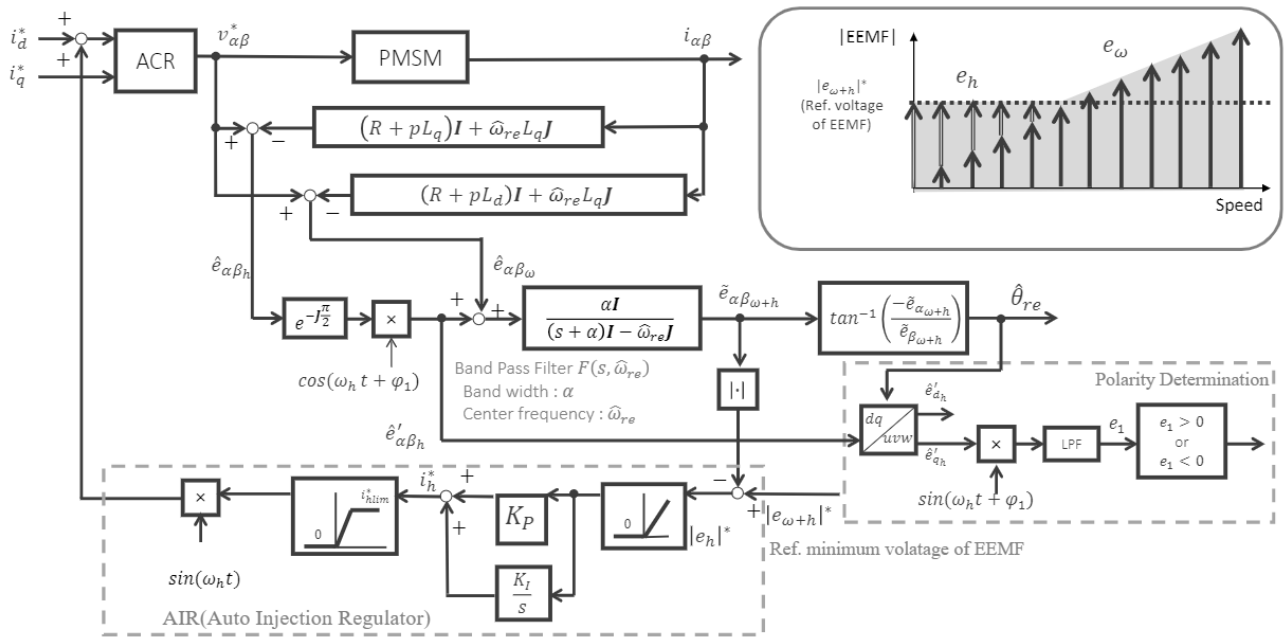

Fig.5 The configuration of $\boldsymbol{EEMF_{\omega+h}}$ position estimator

$$\begin{bmatrix}\hat{e}_{0\alpha}\\ \hat{e}_{0\beta}\end{bmatrix} = \begin{bmatrix}v_\alpha^*\\ v_\beta^*\end{bmatrix} - (R + pL_d)\boldsymbol{I}\begin{bmatrix}i_\alpha\\ i_\beta\end{bmatrix} \quad (5)$$

$$\cong \omega_{re0}K_E\begin{bmatrix}-sin\theta_{re}\\ cos\theta_{re}\end{bmatrix} \quad (6)$$

$$\hat{\omega}_{re0} = \frac{\sqrt{\hat{e}_{0\alpha}^2 + \hat{e}_{0\beta}^2}}{K_E} \quad (7)$$

$\left[\hat{e}_{0\alpha},\ \hat{e}_{0\beta}\right]^T$ in Eq.(5) is the estimated Approximate EMF, and Eq.(7) is the initial speed estimation equation. As shown in Eq.(6), $\boldsymbol{e_0}$ is the approximate value of Back-EMF, and when $v_\alpha^* = v_\beta^* = 0$, the response of $\hat{\omega}_{re0}$ can be calculated regardless of the time constant, and then initial position estimation and the voltage reference can be compensated at flying-start.

However in practice, the initial speed estimation cannot be properly performed just by Eq.(5) and Eq.(7), because of the fluctuation caused by high frequency terms of Back-EMF and the influence of the coordinate transformation. Thus, to avoid the fluctuation, the estimation should be performed on UVW axis like Eq.(9) and Eq.(10), and a filter is needed to suppress the high frequency terms. In this paper, a first order low-pass filter is used in experiments.

$$\begin{bmatrix}\hat{e}_{0u}\\ \hat{e}_{0v}\\ \hat{e}_{0w}\end{bmatrix} = \begin{bmatrix}v_u^*\\ v_v^*\\ v_w^*\end{bmatrix} - \frac{2}{3}\begin{bmatrix}R+pL_q & 0 & 0\\ 0 & R+pL_q & 0\\ 0 & 0 & R+pL_q\end{bmatrix}\begin{bmatrix}i_u\\ i_v\\ i_w\end{bmatrix} \quad (8)$$

$$\hat{\omega}_{re0} = \frac{\sqrt{\hat{e}_{0u}^2 + \hat{e}_{0v}^2 + \hat{e}_{0w}^2}}{\sqrt{\frac{2}{3}}K_E} \quad (9)$$

3. PROPOSED FLYING-START STRATEGY

3.1. Position estimation method

In this paper, position can be estimated seamlessly with a single $EEMF_{\omega+h}$ observer, and the configuration is shown in Fig.5. This basic configuration is a disturbance observer that subtracts impedance's voltage drop and then passes the $\alpha\beta$ coordinate filter. The $EEMF_{\omega+h}$ model is shown below.

$$\begin{bmatrix}v_\alpha\\ v_\beta\end{bmatrix} = \{(R + pL_d)\boldsymbol{I} + \omega_{re}L_q\boldsymbol{J}\}\begin{bmatrix}i_\alpha\\ i_\beta\end{bmatrix} + \begin{bmatrix}e_{\alpha\omega+h}\\ e_{\beta\omega+h}\end{bmatrix} \quad (10)$$

$$\begin{bmatrix}e_{d\omega+h}\\ e_{q\omega+h}\end{bmatrix} = \begin{bmatrix}0\\ \omega_{re}\{(L_d - L_q)i_d + K_E\}\end{bmatrix} + \begin{bmatrix}(L_d - L_q)\dot{i}_d\\ 0\end{bmatrix} \quad (11)$$

$$= e^{-\boldsymbol{J}\omega_{re}t}\begin{bmatrix}e_\alpha\\ e_\beta\end{bmatrix} \quad (12)$$

$$\begin{bmatrix}e_{d\omega+h}\\ e_{q\omega+h}\end{bmatrix} = \begin{bmatrix}e_{d\omega}\\ e_{q\omega}\end{bmatrix} + \begin{bmatrix}e_{dh}\\ e_{qh}\end{bmatrix} \quad (13)$$

$$e^{-\boldsymbol{J}\omega_{re}t} = \begin{bmatrix}cos\omega_{re}t & -sin\omega_{re}t\\ sin\omega_{re}t & cos\omega_{re}t\end{bmatrix}$$

$\left[e_{\alpha\omega+h},\ e_{\beta\omega+h}\right]^T$ in Eq.(10) is voltage vector $EEMF_{\omega+h}$. It contains two vectors in Eq.(13), $EEMF_\omega$ (first term) and $EEMF_h$ (second term). $EEMF_\omega$ is the elements excited proportional to the velocity, used in the middle and high speed range. $EEMF_h$ is the elements excited proportional to the current derivative, which means it can be excited by applying a high-frequency signal injection. In order to generate $EEMF_h$, a sinusoid wave is injected to the d axis current like Eq.(14).

$$\begin{bmatrix}i_{dh}^*\\ i_{qh}^*\end{bmatrix} = |i_h|\sin(\omega_h t)\begin{bmatrix}1\\ 0\end{bmatrix} \quad (14)$$

i_h and ω_h express the injection signal amplitude and injection frequency respectively. In practice, to combine $EEMF_h$ and $EEMF_\omega$ in the q axis, a 90 degree phase transformation is needed, and then $EEMF_{\omega+h}$ in stable is shown as Eq.(15) and Eq.(16).

$$\begin{bmatrix}\tilde{e}_{d_{\omega+h}}\\ \tilde{e}_{q_{\omega+h}}\end{bmatrix} = F(s,\hat{\omega}_{re})\left\{E_\omega + \cos(\omega_h t)\, e^{-\frac{J\pi}{2}} E_h\right\} \quad (15)$$

$$\begin{bmatrix}\tilde{e}_{d_{\omega+h}}\\ \tilde{e}_{q_{\omega+h}}\end{bmatrix} = \begin{bmatrix}0\\ \hat{\omega}_{re}\{(L_d - L_q)i_d + K_E\}\end{bmatrix} + \begin{bmatrix}0\\ \frac{1}{2} i_h \omega_h (L_q - L_d)\end{bmatrix} \quad (16)$$

$F(s,\hat{\omega}_{re})$in Eq.(15) is the bandpass filter with bandwidth α and center frequency$\hat{\omega}_{re}$, where α is determined from the robustness to velocity estimation errors and disturbance suppression characteristics for harmonic disturbances in the EMF waveform by the following formula. μ is a constant, and a certain lower limit is set for α.

$$\alpha = \mu|\hat{\omega}_{re}| \quad (17)$$

While $EEMF_\omega$ cannot ensure sufficient amplitude for estimation in standstill or low speed range, the shortfall can be covered by $EEMF_h$. Thus, the position can be estimated in all speed range by a single $EEMF_{\omega+h}$ extimator.

$$\hat{\theta}_{re} = \tan^{-1}\left(\frac{-\tilde{e}_{\alpha_{\omega+h}}}{\tilde{e}_{\beta_{\omega+h}}}\right) \quad (18)$$

Besides, by setting $|e_{\omega+h}|^*$ which is the minimum amplitude of the $EEMF_{\omega+h}$ for signal detection, auto signal injection regulator (AIR) can automatically calculate the necessary amplitude of i_h during motor-driving to generate $EEMF_h$ in Fig.5. Besides at standstill and low speed, before $EEMF_h$ passing the band pass filter, we take out the q axis term and multiply the signal to estimate the constant term e_1, which can determine the polarity by plus-minus sign, shown in Fig.5.

$$\begin{bmatrix}\hat{e}'_{d_h}\\ \hat{e}'_{q_h}\end{bmatrix} = e^{-J\omega_{re}t}\begin{bmatrix}\hat{e}'_{\alpha_h}\\ \hat{e}'_{\beta_h}\end{bmatrix} \quad (19)$$

$$e_1 = F_{LPF}\left\{\sin(\omega_h t + \phi_1) * \hat{e}'_{q_h}\right\} = \mp\frac{1}{8} L_{d1} i_{h0}^2 \omega_h \quad (20)$$

L_{d1} is the ratio of the current against inductance. By setting the amplitude of the signal injection $i_h^* = i_{h0}$ which is needed for magnetic saturation, $EEMF_{\omega+h}$ can estimate the position and $EEMF_h$ can determine the polarity at the same time.

3.2. Flying-start algorithm with initial speed estimation

The signal injection in high speed range leads to increasing the band width of the band pass filter, which causes the low accuracy of position estimation. Therefore, in the flying-start algorithm, the speed range is determined at first to decide if the signal injection is needed. The flying-start strategy with initial speed estimation is shown as Fig.6. Since $|e_{\omega+h}|^*$ is the minimum amplitude of the $EEMF_{\omega+h}$ for signal detection, we can use it to determine the speed range as well. The method consists of two steps.

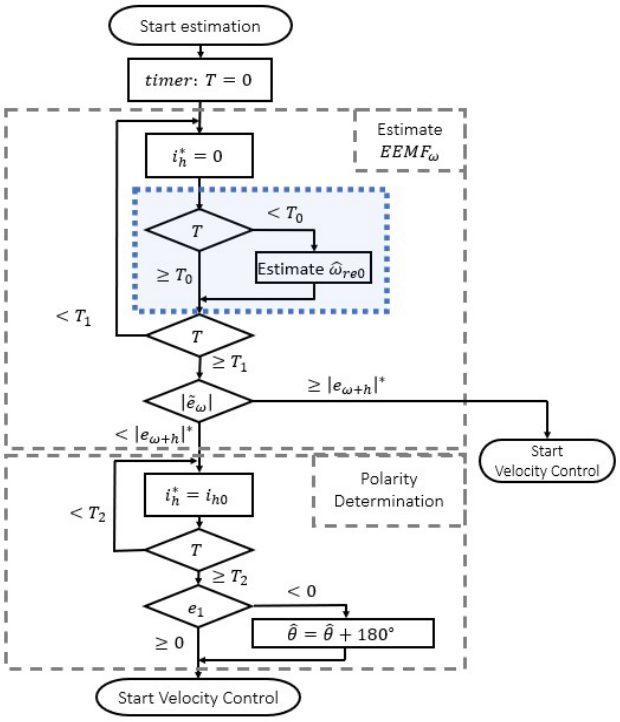

Fig.6 Flying-start strategy with initial speed estimation

Step1: Setting $i_h^* = 0$ to estimate $EEMF_\omega$ only.
Meanwhile, the initial speed $\hat{\omega}_{re0}$ is estimated.

Step2:

(a) If $|EEMF_\omega| \geq |EEMF_h|$,
it means in middle/high speed range
and the polarity determination is unnecessary.
So the initial position can be estimated by $EEMF_\omega$,
and velocity control can start.

(b) If $|EEMF_\omega| < |EEMF_h|$,
it means that it's in low speed range
and the polarity determination is necessary.
So we set $i_h^* = i_{h0}$ to generate $EEMF_h$
and initial position is estimated by $EEMF_{\omega+h}$.
Then velocity control can start.

To avoid the overcurrent, the automatic current regulator generates the current reference as $i_d^* = i_q^* = 0$ when position estimation starts, keeping the dq axis current to zero. With the initial estimated position compensated by initial speed estimation, the voltage reference can be initialized in several carrier period, and decoupling voltage error is compensated quickly to suppress the inrush current.

4. EXPERIMENTS

Table 1 shows the conditions of experimental IPMSM and Table 2 shows the conditions of controller. The time constant of the algorithm in Fig.4 is $T_0 = 3[ms]$, $T_1 = 10[ms]$, $T_2 = 20[ms]$,

Table 1 Conditions of experimental IPMSM

Symbol	Meaning	Value
R	Resistance	0.53Ω
L_d	d-axis Inductance	$4.15mH$
L_q	q-axis Inductance	$16.74mH$
K_E	EMF constant	$0.091V/rad/s$
P_n	Number of Pole pairs	2
I_R	Rated Ampere	$8A$
ω_R	Rated speed	$2500rpm$
V_{DC}	DC-link voltage	$130V$

Table 2 Conditions of Controller

Meaning	Value
Carrier frequency	$5\ kHz$
Current control period	$100\mu s$
Observer control period	$100\mu s$
Speed control period	$1\ ms$
Current response frequency	2000 rad/s
Signal injection frequency ($f_h = \omega_h/2\pi$)	$400\ Hz$
Phase compensation(ϕ_1)	-0.8 rad

which is decided by filters.

Fig. 7 to Fig. 10 show the results when the motor startup speed was regulated at 0%(standstill), 5\%(low speed), 10\%(middle speed),100\%(high speed) of the rated speed with initial speed estimation. Flying-start program is from Time=5[ms], and after the flying start, velocity control starts and velocity reference is 100\% rated speed. $|\hat{e}_0|$ shown in results means the amplitude of estimated Approximate EMF passes the LPF before and after.

Fig. 7 and Fig. 8 presents the startup from standstill and low speed, which needs signal injection after estimating $EEMF_\omega$ in Step 1. In this case, the response of $\hat{\omega}_{re0}$ is small due to S/N duty, but inrush current doesn't occur. That is because the disturbance is small at low speed. Fig.9 and Fig.10 show that signal was not injected in Step 2 for enough $EEMF_\omega$, and the response of $\hat{\omega}_{re0}$ compensate the position estimation and decoupling voltage, suppressing the inrush current. In Fig. 10, even at the rated speed when the risk of the inrush current is largest, the response can decrease to zero before velocity control starts.

4. CONCLUSION

In this paper, the issues on conventional flying-start strategy are discussed, and a flying start strategy with initial speed estimation in overall speed range is proposed as the solution. By conducting

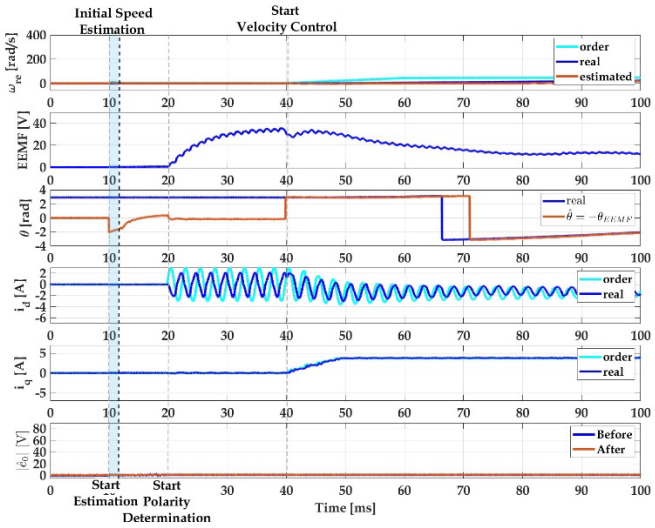

Fig.7 Flying-start from standstill

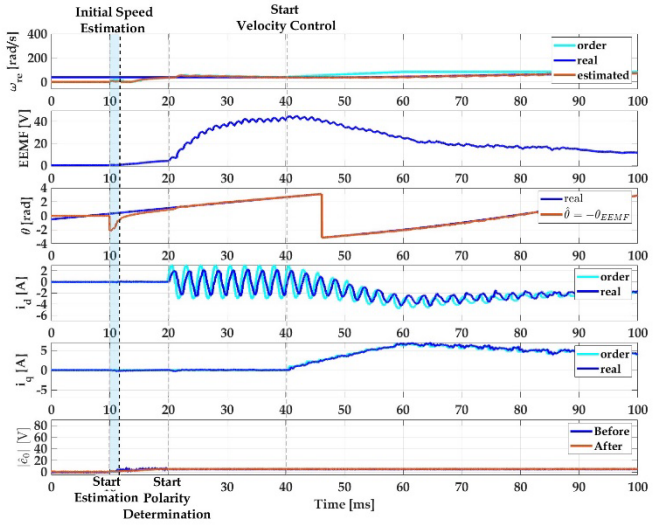

Fig.8 Flying-start from low speed

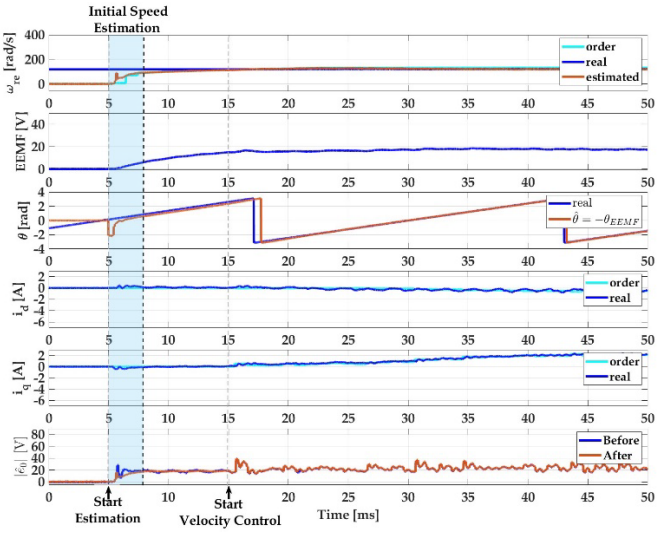

Fig.9 Flying-start from middle speed

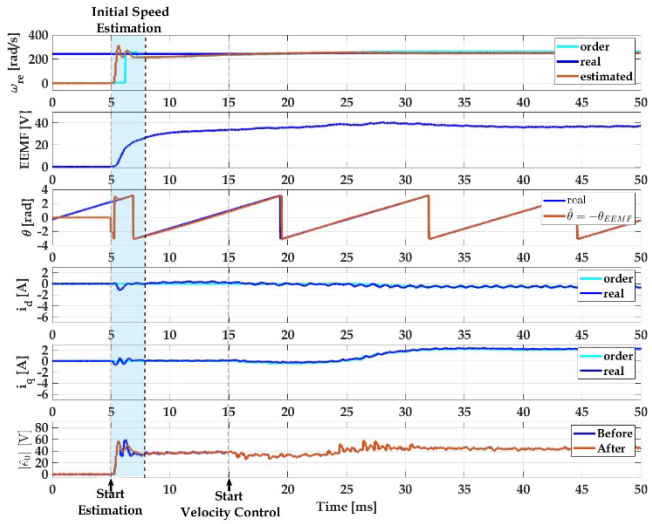

Fig.10 Flying-start from high speed

the performance evaluation experiments on motor bench, it shows that the strategy can flying start the sensorless PMSM at overall speed safely without overcurrent occurring.

REFERENCES

(1) S. Ogasawara, T. Matsuzawa and H. Akagi, “A Position-Sensorless IPM Motor Drive System Using a Position Estimation Based on Magnetic Saliency,” *IEEJ Trans. Ind. Appl.*, Vol. 118, No. 5, pp. 652-660, 1998.(in Japanese)

(2) T. Takeshita, M. Ichikawa, N. Matsui, E. Yamada and R. Mizutani, “Initial Rotor Position Estimation of Sensorless Salient-Pole Brushless DC Motor,” *IEEJ Trans. Ind. Appl.*, Vol. 116, No. 7, pp.736-742, 1996. (in Japanese)

(3) Z. Chen, M. Tomita, S. Doki and S. Okuma, “An Extended Electromotive Force Model for Sensorless Control of Interior Permanent Magnet Synchronous Motors,” *IEEE Trans. Industrial Electronics*, Vol. 50, No. 2, pp. 288-295, 2003.

(4) T. Aihara, A. Toba, T. Yanase, A. Mashimo and K. Endo , “Sensorless Torque Control of Salient-Pole Synchronous Motor at Zero-Speed Operation,” *IEEE Trans. on Power Electronics*, Vol. 50, No. 1, pp. 202-208, 1999.

(5) S. Kondo, S. Doki, A. Matsumoto and M. Tomita , “Analysis about Control Model for Position Sensorless Control of PMSMs based on Expression of Imaginary Electromotive Force,” *IEEJ Transactions on Industry Applications,* Vol. 139, No. 1, pp.1-12, 2019. (in Japanese)

(6) T. C. Lin and Z. Q. Zhu, “Sensorless operation capability of surface-mounted permanent-magnet machine based on high-frequency signal injection methods,” *IEEE Trans. Ind. Appl.*, vol. 51, no. 3, pp. 2161–2171, May/Jun. 2015.

(7) K. Lee, S. Ahmed, and S. M. Lukic, “Universal restart strategy for high-inertia scalar-controlled PMSM drives,” *IEEE Trans. Ind. Appl.*, vol. 52, no. 5, pp. 4001–4009, Sep./Oct. 2016.

(8) R. Hao, T. Kozakura and S. Doki, “Performance Evaluation of Startup and Driving Strategy at Overall Speed with Extended ElectroMotive Force for Position Sensorless Permanent Magnet Synchronous Motor,” *2022 International Power Electronics Conference (IPEC-Himeji 2022- ECCE Asia)*, pp. 362-367, Himeji, Japan, May 15-19, 2022.